Investigating and calculating the temperature of hot-spot factor for transformers

Khalid Yahya[1,5], Hani Attar[2], Haitham Issa[2], Jamal Ali Ramadan Dofan[3], Nassim A. Iqteit[4], Adel E. M. Yahya[5], Ahmed Amin Ahmed Solyman[6]

[1]Department of Electrical and Electronics Engineering, Nisantasi University, Istanbul, Turkey
[2]Department of Energy Engineering, Zarqa University, Zarqa, Jordan
[3]Department of Electrical and Electronics Engineering, Gharian University, Gharyan, Libya
[4]Department of Electrical Engineering, Palestine Polytechnic University, Hebron, Palestine
[5]Department of Electrical Engineering, Sabratah University, Sabratha, Libya
[6]Department of Electrical and Electronic Engineering, Istanbul Gelisim University, Istanbul, Turkey

Article Info

Article history:

Received Jun 5, 2022
Revised Feb 16, 2023
Accepted Feb 18, 2023

Keywords:

Distribution transformer
Tehrmal-electrical metaphor
Temperature loss
Thermal resistance
Transient states

ABSTRACT

This article explores the measurement of temperature in transient states, utilizing the principles of heat transfer and thermal-electrical metaphor. The study focuses on the nonlinear thermal resistances present in various locations within a distribution transformer, while taking into account variations in oil physical variables and temperature loss. Real-time data obtained from heat run tests on a 250-MVA-ONAF cooled unit, conducted by the transformer manufacturer, is used to verify the thermal designs. The observations are then compared to the loading framework of the IEC 60076-7:2005 system. The findings of this research provide a better understanding of temperature measurement in transient states, particularly in distribution transformers, and can be applied to the design and development of more efficient and reliable transformer systems.

Corresponding Author:

Khalid Yahya
Department of Electrical and Electronics Engineering, Nisantasi University
Maslak Mahallesi, Taşyoncası Sokak, No: 1V ve No:1Y Bina Kodu: 34481742, Istanbul, Turkey
Email: khalid.omy@gmail.com and khalid.yahya@nisantasi.edu.tr

1. INTRODUCTION

The significant proportion of infrastructure investment in generation and distribution power stations is characterize by power transformers. Moreover, the transformer is one of the costliest elements of an energy grid as the power transformer disruptions have a significant economic effect on the operation of the transmission grid. Identifying their status is thus important for achieving the objectives of optimizing return on investment and reducing the overall costs related to the operation of the transformer. The warm heating rate is amongst the most model aspects controlling the average lifespan of a transformer. Among the most important metrics in evaluating the life of power transformer is the winding warm temperature, as the highest aging rate happens at the highest point that encounters the greatest temperature. In addition, for the transformer to have a healthy average lifespan, the warm temperature must blow up the allowed maximum amount.

It is commonly acknowledge that for a 6 °C rise in temperature, the insulation loss roughly doubles [1]. An effective warm temperature estimation is thus critical for both suppliers and users. There are a few ways to calculate the temperature; the first is to use fiber optical heating elements located at the windings' that anticipated the warmth. Thermal sensors mounted to the bottom of the fiber optics are normally mount between the isolated connector and the sprocket while their impulses are emit from the tank through the optical fiber. From over decades, major changes resolve the fiber optic being far too brittle and sensitive handling is need.

Precise calculation of warm temperature can be achieve from using this process. The IEEE and IEC loading manuals [2], [3] used to measure the temperature of the warm using heat-run experiment data and analytical variables. In addition, the temperature of the transformer rely on the exact failures in the transformer produced. This implies that the different transformer root and wind losses are important for deciding the winding intensity. The IEEE C.57.120 [4], [5] models can measure transformer losses. Even so, the real losses are required to determine the actual wind level, for example, the losses should be measure based on data. Iqteit and Yahya [6] described an automated transformer loss calculation, which requires a comprehensive measurement operation. Fuchs *et al*. [7] also constructed an enhanced real time tracking system for transformer damages, differentiating among iron core and copper losses. In addition to measuring the iron core, researchers incorporate eddy current and hysteresis loses and then use ohmic wind and stray losses to assess the conduction loss. Nevertheless, another such distinction among ohmic wind and stray losses is important since the stray losses arise in various parts of the transformer [8] and hence have only a slight influence on the intensity of the winding. Consequently, the temperature is primarily influence by losses in ohmic winding [9]–[11].

Figure 1 provides a simple thermal management system for power transformers, for which oil intensity within the windings is supposed to rise linearly from start to end, while the temperature differential here between pipe oil and the winding coil is steady during the winding phase [12], [13]. The change in the warmth temperature is greater than the change in the concentration of the coil at the tip of the wind, which can see in Figure 1 whenever the changes due to stray losses are factor into the equation. Even so, this conventional method of measuring temperature s has found to be insufficient in accordance with the real data recorded by fiber optic sensors [14], [15]. Blume *et al*. [16], [17] noted that there's still a time difference between the rising in top-oil temp as well as the rising in duct oil temp under dynamic loading. The consequence of this effect is that the wind hotspot rate is greater than the “IEEE loading guide clause 7” method, which is expected.

It was introduced in [16] that calculations to accommodate for the oil duct temps, the difference in stator winding with temp, the difference in oil viscosity, the impact of the tap direction, as well as the difference in atmospheric temp (temp) as during load period, that were overlooked in the system of “Clause 7”. These updated calculations have been used in the “IEEE loading guide” [3] as option to the hotspot temperature measurement procedure termed as the “Annex G method”. In this article, a quantitative analysis was perform to measure the hotspot temperature amongst the two techniques specified in the IEEE loading guide [3]. In key findings of continuous load, load demand pattern and short-period overload scenarios, four transformers with various cooling mechanisms of “oil natural air natural (ONAN), oil natural air forced (ONAF), oil forced air forced (OFAF), and oil directed air forced (ODAF)”, the measurements of whom are provide in the appendix section, are being used to test the two approaches. Events of ONAF and OFAF measurement have been confirmed by thermal experiments and [16], [17] calculations. A MATLAB/simulink software was used to analyze the hotspot temperature and the consequential loss-of-life.

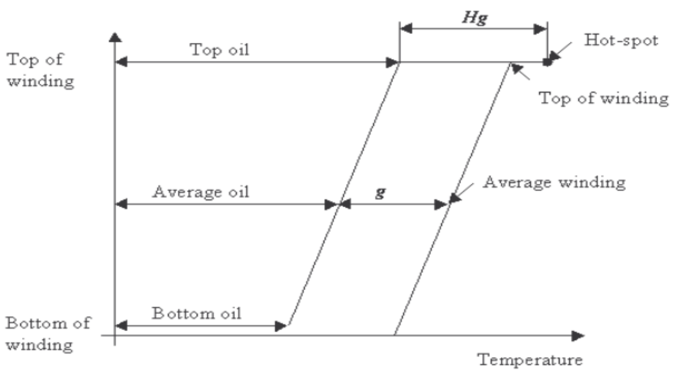

Figure 1. Basic thermal diagram inside the transformer tank [6]

2. TRANSFORMER THERMAL MODELS

The sources from [4]–[8], and [18]–[24] discuss earlier stuff performed in this field of transformer thermal modeling. For all the temperature measurements and wind hotspot forecasts, which have been the IEC and IEEE scientific formulae, the normal approaches followed [18], [19] are inadequate for today's industry competency [20], [21]. Furthermore, basic temperature rise predictions, which have been conducted even now days by the traditional scientific formulae, are not just useful indicators for direct temp calculation or emulation. In an approach to strengthen the precision, further advanced models are now being updated with IEEE and IEC loading guidelines aimed at a fair analysis of the oil temp within the winding, taking into account changes in winding resistance, oil viscosity and oil inertia. The energy balance formula will describe a thermal process.

$$q \times dt = C_{th} \times d\theta + \frac{\theta - \theta_{amb}}{R_{th}} \times dt \tag{1}$$

The given equation includes several variables such as q, C_{th}, θ, Rth, and θ_{amb}. These variables represent the heat generation, thermal capacitance, temperature, thermal resistance, and ambient temperature, respectively. The formula can be interpreted as (2).

$$q = C_{th} \times \frac{d\theta}{dt} + \frac{\theta - \theta_{amb}}{R_{th}} \tag{2}$$

Then, when the describtion a small electronic RC circuit as shown in Figure 2 makes a formula based on both the first principle of Kirchhoff and Ohm.

$$i = C_{el} \times \frac{du}{dt} + \frac{u}{R_{el}} \tag{3}$$

The (3) consists of four distinct variables, i, C_{el}, R_{el}, and u, which represent key components of the electrical system, including electrical current, electrical capacitance, electrical resistance, and electrical voltage, respectively. Merely, we achieve the comparison among electrical and thermal mechanisms by contrasting (3) and (2) as shown in Table 1. Figure 3, the analog thermal circuitry for the electrical process has provided.

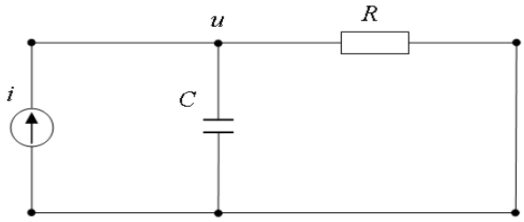

Figure 2. An electrical RC circuit

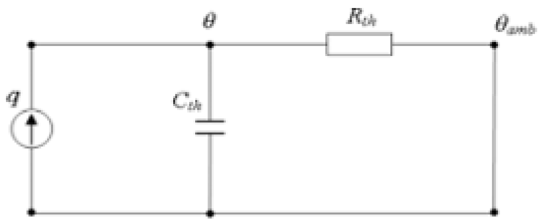

Figure 3. The analogous thermal circuit

Table 1. Thermal-electrical analogy

Thermal		Electrical	
Generated heat	q	Current	i
Temperature	θ	Voltage	u
Resistance	R_{th}	Resistance	R_{el}
Capacitance	C_{th}	Capacitance	C_{el}

2.1. The non-linear thermal resistance

The nonlinear oil thermal resistance, R_{th-oil} $(m^2K)/W$, in accordance with the findings of energy transfer the corresponding formula is express in (4).

$$R_{th-oil} = \frac{1}{h \times A} = \frac{\Delta\theta_{oil}}{q} \tag{4}$$

In the (4), h represents the heat transfer coefficient, A is the area, $\Delta\theta_{oil}$ corresponds to the oil temperature gradient, and q indicates the amount of heat generated by the relevant losses. The natural flow of convection oil across longitudinal, leaned and vertical sheets and tubes can be determined by the following integral approach on the basis of heat transfer theory [14]–[16].

$$N_u = C \times [G_r \times P_r]^n \tag{5}$$

The coefficients C and n depend on whether the oil circulation is laminar or turbulent, and they are obtained empirically. The Nusselt number (N_u), Prandtle number (P_r), and Grashof number (G_r) describe in (3) to (6).

$$N_u = \frac{h \times L}{k} \tag{6}$$

$$P_r = \frac{c_{oil} \times \mu}{k} \tag{7}$$

$$G_r = \frac{L^3 \times \rho_{oil}^2 \times g \times \beta \times (\Delta\theta_{oil})}{\mu^2} \tag{8}$$

Where the L represents the characteristic dimension of the system, which could be the length, width, or diameter of the transformer. The symbol g stands for the gravitational constant, k denotes the thermal conductivity of the transformer oil, ρ_{oil} is the density of the oil, β represents the oil thermal expansion coefficient, c_{oil} is the specific heat of the oil, μ represents the viscosity of the oil, and $\Delta\theta_{oil}$ stands for the oil temperature gradient (K). The continuity equation is achieve by supplementing the (6) to (8) into (5).

$$\frac{h \times L}{k} = C \times \left[\left(\frac{c_{oil} \times \mu}{k}\right) \times \left(\frac{L^3 \times \rho_{oil}^2 \times g \times \beta \times (\Delta\theta_{oil})}{\mu^2}\right)\right]^n \tag{9}$$

Including all transformer isolation oils, it's indeed usually correct that the temp difference of the operating temp is far greater than many of the other oil variables [18]–[20], [25]. It is also possible to substitute all physicochemical characteristics of the oil except perhaps the viscosity in (9) with a standard. Even so, if the effect of all oil variables needs to be weight, the foregoing actions should take. The (10) for the thermal conductivity will be estimate by the following:

$$h = C_1 \times \left(\Delta\theta_{oil} \times \frac{\rho^2 \times \beta \times c_{oil} \times k^{\frac{(1-n)}{n}}}{\mu}\right)^n \tag{10}$$

where $C1$ is assumed to be a constant, and is now expressed as (11).

$$C_1 = C \times \left[g \times L^{\left(\frac{3n-1}{n}\right)}\right]^{(n)} \tag{11}$$

As well as the temp difference of all oil variables is shown by the corresponding equation [20], [21].

$$\mu = A_1 \times e^{\left[\frac{A_2}{\theta_{oil}+273}\right]} \tag{12}$$

$$c_{oil} = A_3 \times A_4\theta_{oil} \tag{13}$$

$$\rho_{oil} = A_5 \times A_6\theta_{oil} \tag{14}$$

$$k = A_7 \times A_8\theta_{oil} \tag{15}$$

$$\beta = A_9 \quad (16)$$

Table 2 lists the nine conditions for the two structural component oils.

Table 2. Insulation oil constants [18], [20]

Oil/constant	Transformer oil	Oil/constant	Transformer oil
A1	0.13573×10^{-5}	A6	-0.659
A2	2797.3	A7	0.124
A3	1960	A8	-1.525x10-4
A4	4.005	A9	8.6x10-4
A5	887		

2.2. The top-oil temp model

As a thermal chain, Figure 4 offers the top-oil temp model. Centered on the principle of heat flow and thermal-electrical analogy [1]–[3], [14]. Where, the total heat generated by losses in a transformer is represented by q_{tot}, with q_{fe} indicating the heat generated by no-load losses and q_l representing the heat generated by load losses. The equivalent thermal capacitance of the transformer oil is denoted by c_{th-oil}, and θ_{oil} represents the top oil temperature. The non-linear oil to air thermal resistance is represented by $R_{th-oil-air}$, and θ_{amb} represents the ambient temperature. Two basic heating elements reflect the heat produced by certain no-load and load transformer falls and the atmospheric temp is described as a value obtained of temp [1], [2]. The nonlinear system seen in Figure 3 for the thermal system is:

$$q_{fe}+q_l=C_{th-oil}\times\frac{d\theta_{oil}}{dt}+\frac{(\theta_{oil}-\theta_{amb})}{R_{th-oil-air}} \tag{17}$$

if we replace the non-linear heat transfer formula (4) with (17), the corresponding model is solved.

$$q_{fe}+q_l=C_{th-oil}\times\frac{d\theta_{oil}}{dt}+\frac{(\theta_{oil}-\theta_{amb})}{\frac{1}{h\times A}} \tag{18}$$

After which, by replacing the thermal conductivity variables for formula (10), h, the differential equation is modified to,

$$(q_{fe}+q_l)\times\frac{\left(\frac{\mu}{\rho^2\times\beta\times c_{oil}\times k^{(1-n)/n}}\right)^n}{C_1\times A}=\frac{\left(\frac{\mu}{\rho^2\times\beta\times c_{oil}\times k^{(1-n)/n}}\right)^n}{C_1\times A}\times C_{th,oil}\times\frac{d\theta_{oil}}{dt}+(\theta_{oil}-\theta_{amb})^{1+n} \tag{19}$$

after that, the parameter can be described as (20)-(24).

$$\mu=\mu_{pu}\times\mu_{rated} \tag{20}$$

$$\rho=\rho_{pu}\times\rho_{rated} \tag{21}$$

$$\beta=\beta_{pu}\times\beta_{rated} \tag{22}$$

$$c=c_{pu}\times c_{rated} \tag{23}$$

$$k=k_{pu}\times k_{rated} \tag{24}$$

As well as the parameters that follow, the measured thermal non-linear instance, $R_{th-oil-air,rated,}$ the measured temp of the top oil rises above the ambient temp, $\Delta\theta_{oil,rated}$:

$$\Delta\theta_{oil,rated}=\left(q_{fe}+q_l\right)_{rated}\times R_{th-oil-air,rated} \tag{25}$$

$The\ rated\ top-oil\ time\ constant, \tau\_(oil, rated).$

$$\tau_{oil,rated}=R_{th-oil-air,rated,}\times C_{th-oil,rated} \tag{26}$$

The proportion of load losses to no-load losses at nominal current, R,

$$R=\frac{q_l}{q_{fe}} \tag{27}$$

and the load factor, *K*.

$$K=\frac{I}{I_{rated}} \tag{28}$$

Then expression (19) is simplified to its exact from (29).

$$\frac{1+R+K^2}{1+R}\times\left(\frac{\mu_{pu}}{\rho_{pu}^2\times\beta_{pu}\times c_{oil,pu}\times k_{pu}^{(1-n)/n}}\right)^n\times\Delta\theta_{oil,rated}=\left(\frac{\mu_{pu}}{\rho_{pu}^2\times\beta_{pu}\times c_{oil,pu}\times k_{pu}^{(1-n)/n}}\right)^n\times\tau_{oil,rated}\times\frac{d\theta_{oil}}{dt}+\frac{(\theta_{oil}-\theta_{amb})^{1+n}}{\Delta\theta_{oil,rated}^n} \tag{29}$$

2.3. The hot-spot temp model

The comparison of non-linear opposition here between protective coating surface and the wind surface, the hotspot temp method, which would be centered on the top oil temp will be established. The framework is founded on the principle of traditional energy transfer. The hot-spot temp model is also depicted as a spectral network, comparable to the traditional heat transfer practice for the top-oil temp framework and the non-linear heat capacity as Figure 5 shows [1], [2].

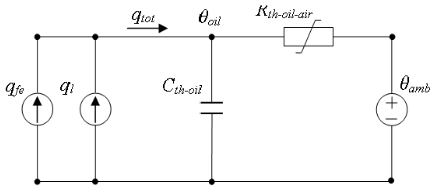

Figure 4. The top-oil temp model

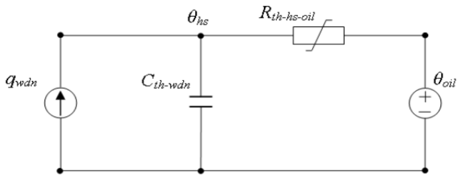

Figure 5. The hot-spot temperature model

The parameters in the figure include q_{wdn}, which represents the heat generated by winding losses, C_{th-wdn}, which is the thermal capacitance of the winding, θ_{hs}, which is the hot-spot temperature, $R_{th-hs-oil}$, which is the nonlinear thermal resistance between the winding and the oil, and θ_{oil}, which is the temperature of the top oil. The vibrational wind is determined using an expression for oil thermal conductivity.

$$R_{th-hs-oil} = R_{th-wdn} + R_{th-insul} + R_{th-insul-oil} \tag{30}$$

The thermal resistances used in the model include the winding thermal resistance R_{th-wdn}, winding insulation thermal resistance $R_{th-insul}$, and non-linear winding insulation to oil thermal resistance $R_{th-insul-oil}$. By comparing the resistances provided in (30), the properties of the transformer can be analyzed:

$$R_{th-insul-oil} \gg R_{th-wdn} \tag{31}$$

$$R_{th-insul-oil} \gg R_{th-insul} \tag{32}$$

for the warm conditions recorded on the insulation's outermost layer twisted across the conductors [22], [23]. The critical value for the nonlinear wind to thermal conductivity of oil is therefore:

$$R_{th-hs-oil} = \frac{1}{h \times A} \tag{33}$$

for both the top oil temp framework, the expression (27) is identical to (4), so the coefficient for the temp profile, h, is completely equivalent to the temp profile in (10).

$$h = C_1 \times \left(\Delta\theta_{oil} \times \frac{\rho^2 \times \beta \times c_{oil} \times k^{\frac{(1-n)}{n}}}{\mu}\right)^n \tag{34}$$

In which all the parameters of the oil are reassessed at the top temp of the oil and $\Delta\theta_{hs}$ is now the hot-spot to top-oil temp gradient. The nonlinear system is shown Figure 4 for the thermal circuitry is:

$$q_{wdn} = C_{th-wdn} \times \frac{d\theta_{hs}}{dt} + \frac{(\theta_{hs} - \theta_{oil})}{R_{th-hs-oil}} \tag{35}$$

if the non-linear thermal conductivity model replaced (34), with (35), the corresponding model is solved.

$$q_{wdn} = C_{th-wdn} \times \frac{d\theta_{hs}}{dt} + \frac{(\theta_{hs} - \theta_{oil})}{\frac{1}{h \times A}} \tag{36}$$

After which, by replacing the thermal conductivity expression, (34) with (36), the dynamic model is modified to:

$$q_{wdn} \times \frac{\left(\frac{\mu}{\rho^2 \times \beta \times c_{oil} \times k^{(1-n)/n}}\right)^n}{C_1 \times A} = \frac{\left(\frac{\mu}{\rho^2 \times \beta \times c_{oil} \times k^{(1-n)/n}}\right)^n}{C_1 \times A} \times C_{th-wdn} \times \frac{d\theta_{hs}}{dt} + (\theta_{hs} - \theta_{oil})^{1+n} \quad (37)$$

The average hot-spot non-linear to top-oil thermal conductivity, $R_{th-hs-oil,rated}$, The measured hot-spot temp rises above the temp of the top oil, $\Delta\theta_{hs,rated,}$ as shown in (38).

$$\Delta\theta_{hs,rated,} = q_{wdn,rated} \times R_{th-hs-oil,rated} = H \times g_r \quad (38)$$

Whereas the hot-spot factor H and the rated average winding to average oil temp gradient g_r are defined in reference [24]. The rated winding time constant $\tau_{wdn,rated,}$, is:

$$\tau_{wdn,rated,} = R_{th-hs-oil,rated}, \times C_{th-wdn,rated} \quad (39)$$

$$p_{wdn,pu}(\theta_{hs}) = p_{dc,pu} \times \left(\frac{\theta_{hs}+\theta_k}{\theta_{hs,rated}+\theta_k}\right) + p_{eddy,pu} \times \left(\frac{\theta_{hs,rated}+\theta_k}{\theta_{hs}+\theta_k}\right) \quad (40)$$

where, $P_{dc,pu}(\theta_{hs})$ and $P_{eddy,pu}(\theta_{hs})$ The activity of the DC and eddy drops is defined as a temp function, the DC losses vary with the temperature directly, while the eddy losses vary with the temp inverse proportion. θ_k It is the loss adjustment temperature variable, equivalent to 225 for aluminum and 235 for copper. It implies that the definitive formula is:

$$\{k^2 \times p_{wdn,pu}(\theta_{hs})\} \times \left(\frac{\mu_{pu}}{\rho_{pu}^2 \times \beta_{pu} \times c_{oil,pu} \times k_{pu}^{(1-n)/n}}\right)^n \times \Delta\theta_{hs,rated} = \left(\frac{\mu_{pu}}{\rho_{pu}^2 \times \beta_{pu} \times c_{oil,pu} \times k_{pu}^{(1-n)/n}}\right)^n \times \tau_{hs,rated} \times \frac{d\theta_{hs}}{dt} + \frac{(\theta_{hs}-\theta_{oil})^{1+n}}{\Delta\theta_{hs,rated}^n} \quad (41)$$

the effect of capacitors that may optimize the maximum electrical power saving is shown in [26], where [27] calculates the transformer minimum energy loss.

3. SIMULATION MODEL

In MATLAB/simulink, the thermal coefficients are patterned. The coefficients are solved simultaneously using the system of Runge-Kutta. The requisite variables for the model are based on data obtained from the standard heat run test carried out by the supplier of the transformer. Each one phase the formula of the top oil model (29) is resolved by K, $\mu_{pu}, \rho_{pu}, \beta_{pu}, c_{oil,pu}, k_{pu} and\ \theta_{amb}$ are the input variable while θ_{oil} The output vector, although both are time constants, is t. Figure 6 presents a schematic diagram of the thermal model for measuring temperature during transient states in a distribution transformer. The applied top oil design is demonstrated in Figure 6(a).

As seen in the condensed Figure 6(b), the measured top oil temp is the input atmospheric temp for the hot spot method. Each one phase the formula of the top oil model (29) is resolved by K, $\mu_{pu}, \rho_{pu}, \beta_{pu}, c_{oil,pu}, k_{pu}, P_{wdn,pu}(hs)\ and\ \theta_{oil}$ are the input variable while θ_h the output vector, although both are time constants, is t. And use the block diagram seen in Figure 7, the applied top oil design is demonstrated.is the output variable which all are functions of time, t.

Where $Q1 = \frac{1+R+K^2}{1+R} \times \left(\frac{\mu_{pu}}{\rho_{pu}^2 \times \beta_{pu} \times C_{oil,pu} \times k_{pu}^{\frac{(1-n)}{n}}}\right)^n \times \Delta\theta_{(oil,rated)}$

$$Q2 = \frac{1}{\left(\frac{\mu_{pu}}{\rho_{pu}^2 \times \beta_{pu} \times C_{oil,pu} \times k_{pu}^{\frac{(1-n)}{n}}}\right)^n \times \tau_{(oil,rated)}}$$

$$Q3 = k^2 \times P_{wdn,pu}(\theta_{hs}) \times \left(\frac{\mu_{pu}}{\rho_{pu}^2 \times \beta_{pu} \times C_{oil,pu} \times k_{pu}^{\frac{(1-n)}{n}}}\right)^n \times \Delta\theta_{(hs,rated)}$$

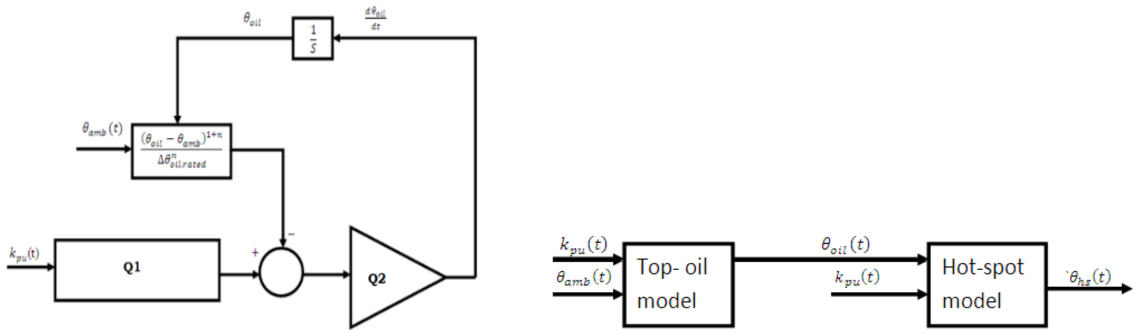

(a) (b)

Figure 6. The schematic diagram model: (a) block diagram of top oil model and (b) simplified diagram of the thermal model

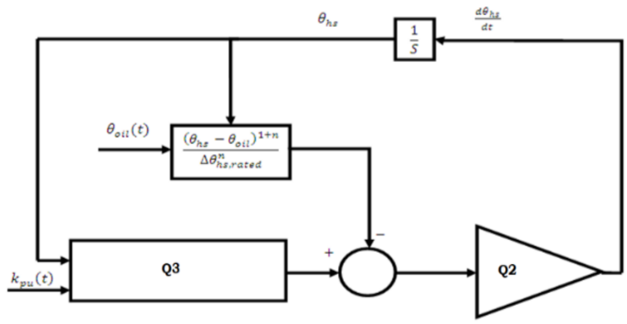

Figure 7. Block diagram of hot spot model

4. SIMULATION RESULATS

This section presents the temperature results obtained from three different transformer modules and various types of tanks during various load tests. These results were obtained using equations (29) and (41) and were compared to the IEC 60076-7:2005 loading guide method. The data used in this analysis was derived from the normal heat training session conducted by the transformer company.

4.1. Transformers with external cooling

Winding temperature restricts the loading of the transformer, so the temperature of the power transformer must maintain beyond a certain boundaries prescribed by regulatory requirements for maximum load and normal ambient temperature. The inrush current temperature is not standardized, and the decentralized control is usually the winding's elevated temperatures portion, named the winding hot spot temperature. The insulated temperature is the key element in the ageing of the transformer. The sheet separation is translocated with the temperature and time reflecting the end of the insulated materials' operation, which is known as the terminal phase of the transformer.

Table 3. The load steps for the 250 MVA transformer

Time period (minutes)	Load
0.0-187.4	1.0
187.4-364.9	0.6
364.9-503.4	1.5
503.4-710.0	0.3
710.0-735.0	2.1
735.0-750.0	0.0

Figure 8 shows the rated impedances for the 250 MVA transformer, which were 230±8 x 1.5 percent/118/21 kV. Figure 8(a) and Figure 8(b) illustrate the load steps for the transformer as presented in Table 3. The oil flow through the 118 kV and 230 kV windings was directed in a zigzag pattern by oil directing circles. The top-oil temperature is presented in Figure 9.

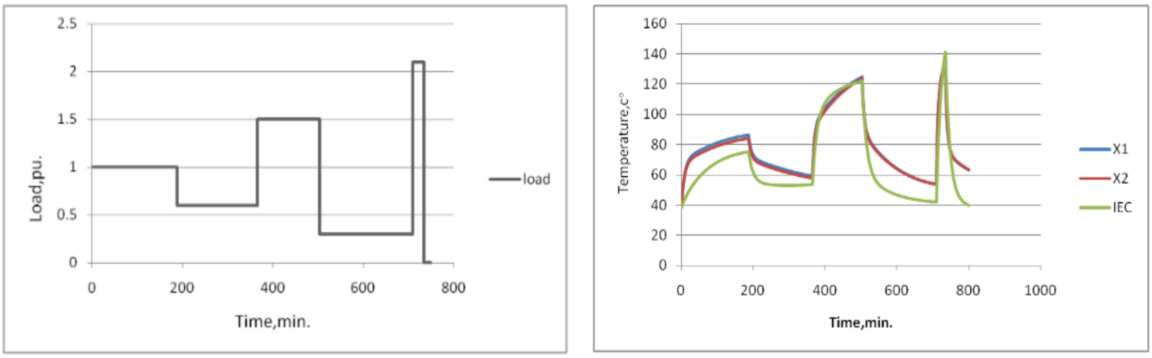

(a) (b)

Figure 8. Load steps and hot-spot temperature of the 250 MVA ONAF-cooled transformer: (a) load steps and (b) hot-spot temperature of the 118 kV winding

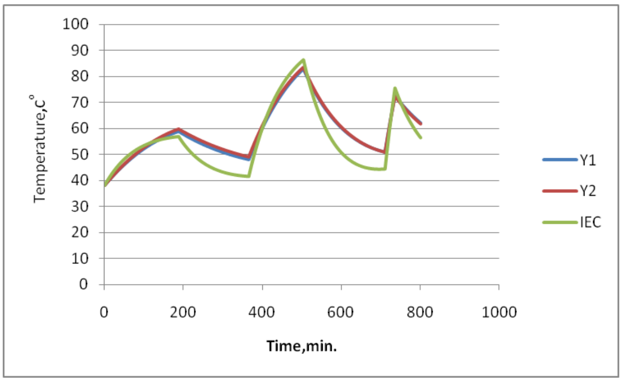

Figure 9. The top-oil temperature of the 250 MVA ONAF-cooled transformer

5. CONCLUSION

This article analyzes an effort by the established thermal electric comparison approach to analyze the specific hot-spot temperature physical analysis for more detailed temperature measurements during load variations. The specific thermal model for the top-oil is often analyzed by the thermal electrical analogy approach used, taking into account the influence of atmospheric temperature on the top-oil temperature. The constants (n) used to define the spectral gradient for the top oil numerical simulation model and the hot spot thermal model are crucial for different cooling mechanisms and transformer architectures. These models were defined in the equations used throughout this research. In the numerical simulation, both oil variable modification and loss variance with temperature are taken into consideration. The findings acquired by the numerical simulation take into consideration of all variations in oil physical variables and the difference in loss with temperature is in fair accordance with the findings plotted by the thermal model. The results stated that, it is worth noting that the IEC 60076-7:2005 loading guide method results less well with the results obtained by thermal model.

REFERENCES

[1] D. Susa, M. Lehtonen, and H. Nordman, "Dynamic thermal modeling of distribution transformers," *IEEE Transactions on Power Delivery*, vol. 20, no. 3, pp. 1919–1929, Jul. 2005, doi: 10.1109/TPWRD.2005.848675.

[2] G. Swift, T. S. Molinski, and W. Lehn, "A fundamental approach to transformer thermal modeling. I. Theory and equivalent circuit," *IEEE Transactions on Power Delivery*, vol. 16, no. 2, pp. 171–175, Apr. 2001, doi: 10.1109/61.915478.

[3] T. L. Bergman, A. S. Lavine, F. P. Incropera, and D. P. DeWitt, *Fundamentals of Heat and Mass Transfer*. Wiley, 2018.

[4] "IEEE guide for loading mineral-oil-immersed transformers," 1995, doi: 10.1109/IEEESTD.1995.8684643.

[5] "Power transformers-part 7 :loading guide for oil-immersed power transformers," *IEC 60076-7:2018*, 2018.

[6] N. A. Iqteit and K. Yahya, "Simulink model of transformer differential protection using phase angle difference based algorithm," *International Journal of Power Electronics and Drive Systems (IJPEDS)*, vol. 11, no. 2, pp. 1088–1098, Jun. 2020, doi: 10.11591/ijpeds.v11.i2.pp1088-1098.

[7] E. F. Fuchs, T. Stensland, W. M. Grady, and M. Doyle, "Measurement of harmonic losses of pole transformers and single-phase induction motors," in *Proceedings of 1994 IEEE Industry Applications Society Annual Meeting*, 1994, pp. 128–134, doi: 10.1109/IAS.1994.345488.

[8] L. Kralj and D. Miljavec, "Stray losses in power transformer tank walls and construction parts," in *The XIX International Conference on Electrical Machines - ICEM 2010*, Sep. 2010, pp. 1–4, doi: 10.1109/ICELMACH.2010.5607891.
[9] R. F. Hassan and K. R. Hameed, "Design of high frequency transformers in different shape of core using matlab program," *Indonesian Journal of Electrical Engineering and Computer Science (IJEECS)*, vol. 20, no. 3, pp. 1159–1172, Dec. 2020, doi: 10.11591/ijeecs.v20.i3.pp1159-1172.
[10] M. M. Marei, M. H. Nawir, and A. A. R. Altahir, "An improved technique for power transformer protection using fuzzy logic protective relaying," *Indonesian Journal of Electrical Engineering and Computer Science (IJEECS)*, vol. 22, no. 3, pp. 1754–1760, Jun. 2021, doi: 10.11591/ijeecs.v22.i3.pp1754-1760.
[11] N. F. M. Yasid, A. A. Alawady, M. F. M. Yousof, M. A. Talib, and M. S. Kamarudin, "The effect of short circuit fault in three-phase core-typed transformer," *International Journal of Power Electronics and Drive Systems (IJPEDS)*, vol. 11, no. 1, pp. 409–416, Mar. 2020, doi: 10.11591/ijpeds.v11.i1.pp409-416.
[12] K.-H. Park, H.-J. Lee, and S.-C. Hahn, "Finite-element modeling and experimental verification of stray-loss reduction in power transformer tank with wall shunt," *IEEE Transactions on Magnetics*, vol. 55, no. 12, pp. 1–4, Dec. 2019, doi: 10.1109/TMAG.2019.2940825.
[13] S. S. Sami, Z. A. Obaid, M. T. Muhssin, and A. N. Hussain, "Detailed modelling and simulation of different DC motor types for research and educational purposes," *International Journal of Power Electronics and Drive Systems (IJPEDS)*, vol. 12, no. 2, pp. 703–714, Jun. 2021, doi: 10.11591/ijpeds.v12.i2.pp703-714.
[14] C. W. Rice, "Free and forced convection of heat in gases and liquids," *Journal of the American Institute of Electrical Engineers*, vol. 42, no. 12, pp. 1288–1293, Dec. 1923, doi: 10.1109/JoAIEE.1923.6593412.
[15] M. Inoue and T. Koyanagawa, "Thermal simulation for predicting substrate temperature during reflow soldering process," in *Proceedings Electronic Components and Technology, 2005. ECTC '05.*, 2005, vol. 2, pp. 1021–1026, doi: 10.1109/ECTC.2005.1441396.
[16] L. F. Blume, A. Boyajian, G. Camilli, T. C. Lennox, S. Minneci, and V. M. Montsinger, *Transformer engineering*, 1st ed. New York: John Wiley & Sons, 1938.
[17] L. F. Blume, A. Boyajian, G. Camilli, T. C. Lennox, S. Minneci, and V. M. Montsinger, *Transformer engineering*, 2nd ed. New York: John Wiley & Sons, 1951.
[18] K. Karsai, D. Kerenyi, and L. Kiss, *Large power transformers*. New York: Elsevier, 1987.
[19] L. W. Pierce, "An investigation of the thermal performance of an oil filled transformer winding," *IEEE Transactions on Power Delivery*, vol. 7, no. 3, pp. 1347–1358, Jul. 1992, doi: 10.1109/61.141852.
[20] L. W. Pierce, "Predicting liquid filled transformer loading capability," *IEEE Transactions on Industry Applications*, vol. 30, no. 1, pp. 170–178, 1994, doi: 10.1109/28.273636.
[21] W. Lampe, L. Pettersson, C. Ovren, and B. Wahlstrom, *Hot-spot measurements in power transformers*. 1984.
[22] *Proceedings of the 30th Session, 29th August-6th September 1984*. International Conference on Large High Voltage Electric Systems, 1984.
[23] H. Nordman and M. Lahtinen, "Thermal overload tests on a 400-MVA power transformer with a special 2.5-p.u. short time loading capability," *IEEE Transactions on Power Delivery*, vol. 18, no. 1, pp. 107–112, Jan. 2003, doi: 10.1109/TPWRD.2002.807747.
[24] "Power transformers - part 7: loading guide for oil-immersed power transformers," *IEC 60076-7:2005*.
[25] R. Grubb, M. Hudis, and A. Traut, "A transformer thermal duct study of various insulating fluids," *IEEE Transactions on Power Apparatus and Systems*, vol. PAS-100, no. 2, pp. 466–473, Feb. 1981, doi: 10.1109/TPAS.1981.316903.
[26] A. Agha, H. Attar, A. Alfaoury, and M. R. Khosravi, "Maximizing electrical power saving using capacitors optimal placement," *Recent Advances in Electrical & Electronic Engineering (Formerly Recent Patents on Electrical & Electronic Engineering)*, vol. 13, no. 7, pp. 1041–1050, Nov. 2020, doi: 10.2174/2352096513666200212103205.
[27] A. Agha, H. Attar, and A. K. Luhach, "Optimized economic loading of distribution transformers using minimum energy loss computing," *Mathematical Problems in Engineering*, vol. 2021, pp. 1–9, Dec. 2021, doi: 10.1155/2021/8081212.

BIOGRAPHIES OF AUTHORS

Khalid Yahya received the Ph.D. degree in electrical engineering from Kocaeli University, Kocaeli, Turkey, in 2018. He is currently working as an Assistant Professor of Electrical and Electronics Engineering, Nisantasi University, Istanbul, Turkey. He has published over a dozen articles in prestigious journals and conferences. He is an active reviewer of many conferences and journals. His current research interests include microelectronic circuit analysis and design, renewable energy resources, power electronics, and MPPT designs for energy harvesting systems and information security. He can contact at email: khalid.yahya@nisantasi.edu.tr, khalid.omy@gmail.com.

Hani Attar received his Ph.D. from the Department of Electrical and Electronic Engineering, University of Strathclyde, United Kingdom in 2011. Since 2011, he has been working as a researcher of electrical engineering and energy systems. Dr. Attar is now a university lecturer at Zarqa University, Jordan. His research interests include network coding, wireless sensor networks, and wireless communications. He can contact at email: hattar@zu.edu.jo.

Haitham Issa received his Ph.D. in Communications and Information systems from Zhejiang University, Hangzhou, China, in 2002. He is currently teaching in the Department of Electrical Engineering in Zarqa University, Zarqa, Jordan. His current research interests include image processing, signal Processing, pattern recognition, machine learning, electronics, communication, and renewable energy. He can contact at email: hissa@zu.edu.jo.

Jamal Ali Ramadan Dofan received the master degree in electrical engineering from UTHM University, Johor, Malaysia, in 2011. He is currently working as an Assistant Professor of Department of Electrical and Electronics Engineering, Gharian University, Libya. His current research interests include high voltage, renewable energy, and electrical machine. He can contact at email: jamlgsm@gmail.com.

Nassim A. Iqteit was born in 1983 in Hebron, Palestine. He received a B.Sc. degree in Industrial Automation Engineering from Palestine Polytechnic University (PPU), Palestine, in 2006 and his M.Sc. degree in Electric Power Engineering from Yarmouk University, Jordan, in 2011, and his Ph.D. degree in Electrical Power Engineering from Kocaeli University, Kocaeli, Turkey. He Assistant professor in Electrical Engineering Department at Palestine Polytechnic University, Palestine. His research interests include SEIG modeling, applications of DGs, and distribution system modeling. Integrating renewable energy resources and electrical vehicles with smart grids. He can contact at email: nassim_eng83@ppu.edu.

Adel E. M. Yahya received the Ph.D degree in electrical engineering from Slovak University of Technology in Bratislava, Slovakia. He is currently working as an Associate Professor of Department of Electrical and Electronics Engineering, Gharian University, Libya. His current research interests include high voltage, renewable energy resources, and power electronics. He can contact at email: adel.yahya@sabu.edu.ly.

Ahmed Amin Ahmed Solyman received the Ph.D. degree from the University of Strathclyde, U.K., in 2013. He is currently an Assistant Professor with the Department of Electrical and Electronics Engineering, Istanbul Gelisim University, Turkey. His research interests contain wireless communication networks, IoT, and MIMO communication systems. He can contact at email: aaasahmed@gelisim.edu.tr.